

www.acsami.org Research Article

Finely Designed P3HT-Based Fully Conjugated Graft Polymer: Optical Measurements, Morphology, and the Faraday Effect

Xunshan Liu, Emigdio E. Turner, Valerii Sharapov, Dafei Yuan, Mohammad A. Awais, Jeffrey J. Rack,* and Luping Yu*



Cite This: ACS Appl. Mater. Interfaces 2020, 12, 30856-30861



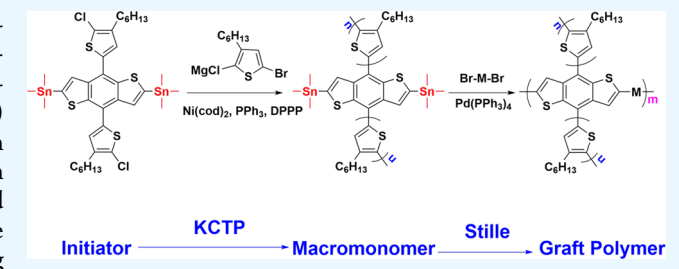
ACCESS

Metrics & More

Article Recommendations

Supporting Information

ABSTRACT: In this work, our group synthesized and characterized a fully conjugated graft polymer comprising of a donor–acceptor molecular backbone and regioregular poly(3-hexylthiophene) (RRP3HT) side chains. Here, our macromonomer (MM) was synthesized via Kumada catalyst transfer polycondensation reaction based on ditin-benzodithiophene (BDT) initiator. The tin content of MM was then investigated by inductively coupled plasma-mass spectrometry (ICP-MS), which allowed for accurate control of donor/acceptor monomer ratio of 1:1 for the following Stille coupling polymerization toward our graft polymer (BP). The



structures of the polymers were then characterized by gel permeation chromatography (GPC), NMR, and elemental analysis. This was followed by the characterization of optical, electrochemical, and physical properties. The magneto-optical activity of graft polymer **BP** was then measured. It was found that, despite the presence of the acceptor backbone, the characteristic large Faraday rotation of RRP3HT was maintained in polymer **BP**, which exhibited a Verdet constant of $2.39 \pm 0.57 (10^4)$ °/T·m.

KEYWORDS: synthesis, conjugated grafting polymer, grafting through, P3HT, Faraday effect

1. INTRODUCTION

Architectural design and control of polymer structures is a continuously pursued research effort. One is looking for new properties from different structures because the function could also follow form. Recent years have witnessed a rapid development of numerous organic semiconducting polymers for applications in a wide range of areas. 1-3 Among these, donor-acceptor copolymers have been extensively investigated. While the majority of efforts have been devoted toward developing new building blocks for these polymers, developing novel chemistry to synthesize new architectures of conjugated polymers has been seldom reported. For instance, developing fully conjugated graft copolymers comprising of different types of polymers in the backbone and side chains has been rarely reported. 4,5 The ability to combine two kinds of polymers with different properties in a single graft polymeric system offers potentials not available in each individual material.6-8

To the best of our knowledge, there are only two papers to have studied conjugated graft polymers that may be because of some inherent limitations of these two methods. Kumada catalyst transfer polycondensation (KCTP) has been widely used for synthesizing graft polymers. Previous studies have already demonstrated both "grafting from" and "grafting through" methods for synthesizing fully conjugated graft polymers employing KCTP polymerization. As for the grafting from method, the functionalized reactive sites on the

molecular backbone may be not active enough to initiate the growth of the side chains because of the electrical properties of the backbone. 11 Second, the side chains may grow randomly and thus causing differences in the degree of polymerization (DP). Third, it is almost impossible to ensure that all of the active sites along the molecular backbone are fully reacted, and thus generating structural defects. For the grafting through method, a macromonomer with two functional groups is prepared for copolymerization. However, since the macromonomer's molecular weight is not fixed (different lengths for side chains), one can only roughly estimate the number of the functional groups by NMR or gel permeation chromatography (GPC) and hence making it impossible to control a 1:1 ratio for the two monomers leading to a low degree of polymerization.4 Another key reason of limited developments in this field might be the lack of related applications. The reported graft polymers did not show promising properties for their potential application. For example, the authors tried to apply these materials to organic field-effect transistors; however, the obtained charge mobilities were too low for good device

Received: May 4, 2020 Accepted: June 15, 2020 Published: June 15, 2020





performance. Therefore, a well-designed method to synthesize polymers with high DP, less traps, and fixed side chain length is needed; appropriate applications for this kind of materials are demanded.

In this work, we developed a new method for synthesizing fully conjugated graft polymers (BP), as shown in Figure 1. A

A grafting through approch towards a fully conjugated brush polymer

Figure 1. Synthetic routes for the brush polymer.

ditin-benzodithiophene (BDT) unit with two chlorothiophenes as pendant groups was functionalized with two trimethyltin groups. Then, regioregular P3HT (RRP3HT) chains were grown from the chlorothiophene unit by the KCTP method to yield a macromonomer ($\mathbf{M}\mathbf{M}$) showing a low polydispersity index ($\mathbf{\mathcal{D}}$) of 1.25. The trimethyltin groups survived the Kumada condition, and the tin content of $\mathbf{M}\mathbf{M}$ was investigated with inductively coupled plasma-mass spectrometry (ICP-MS) allowing us to accurately control the

ratio of **MM** to the other monomer for the Stille polycondensation. The structures of the resulting brush polymers were investigated, and their thermal, photophysical, and electrochemical properties were studied. More importantly, a new application, Faraday rotation, induced by polymer **BP** was investigated. It was found that the regioregular P3HT side chains in polymer **BP** maintained the large magneto-optical activity previously demonstrated for pure RRP3HT. The specific packing morphology of RRP3HT that yields large magneto-optical activity is still a subject of on-going study. ^{12–15} Furthermore, the effect of an acceptor domain on the thin-film "giant Faraday rotation" has previously not been studied. The maintained Faraday rotation implies that the packing of RRP3HT side chains forms extended domains, which exhibit properties similar to pure RRP3HT.

2. RESULTS AND DISCUSSION

2.1. Synthesis and Characterization. The polymer structure and synthetic route are shown in Scheme 1. The structures of the monomers and copolymers were confirmed by 1 H NMR, matrix-assisted laser desorption ionization time-of-flight (MALDI-TOF), and elemental analysis. The two polymers exhibited excellent solubility in common organic solvents such as chloroform, tetrahydrofuran (THF), and chlorobenzene. Table 1 summarizes the polymerization results and thermal properties of the copolymers. The molecular weights (M_w) and D of the two copolymers were $M_w = 16.9$

Scheme 1. Synthetic Routes of the Macromonomer and Brush Copolymer

Table 1. Polymerization Results and Thermal Properties of Copolymers

copolymers	yields (%)	$M_{\rm n}$	$M_{\rm w} ({\rm kg \cdot mol}^{-1})^a$	Đ	$T_{\rm d} ({}^{\circ}{\rm C})^{b}$
MM	87	13.5	16.9	1.25	352
BP	83	39.5	102.0	2.58	386

^aDetermined by GPC in THF based on polystyrene standards. ^bDecomposition temperature, determined by TGA in nitrogen, based on 5% weight loss.

kg/mol with a $\mathcal{D}=1.25$ for MM and $M_{\rm w}=102.0$ kg/mol with a $\mathcal{D}=2.58$ for BP, as determined by gel permeation chromatography (GPC) using polystyrenes standard and CHCl₃ as the eluent. The thermal properties of the copolymers were determined by thermogravimetric analysis (TGA) under a nitrogen atmosphere at a heating rate of 10 °C/min. The two polymers (MM and BP) showed good thermal stability with onset decomposition temperatures ($T_{\rm d}$) corresponding to a 5% weight loss at 352 and 386 °C, respectively, as shown in Table 1.

The synthesis of the macromonomer via KCTP is the crucial step in our synthesis. Normally, this polymerization is quenched with HCl; however, since the macromonomer has trimethyltin groups attached that are sensitive to acidic conditions, the reaction was just quenched with MeOH. NMR spectrum (Figure S6) of MM showed a clear signal at 0.43 ppm, which is consistent with the trimethyltin signal of the initiator compound 4 at 0.41 ppm (Figure S4). The integration ratio of the methyl groups with the aromatic protons on the thiophenes indicated that the DP of the P3HT chains is around 20, which is in good agreement with the starting material ratio of the thiophene Grignard reagents and the initiator of 38. Theoretically, each side of the BDT unit should attach 19 thiophenes, plus one from the initiator itself totaling 20. ICP-MS was employed to investigate the tin content that was found to be 2.13% by weight. With this result, we were able to control the amount of the monomer compound 6 to keep a 1:1 ratio, which is a crucial issue that previous studies were unable to solve. Then, graft polymer BP was obtained that showed a relatively high DP of around 3, which is higher than the published work with grafting through method.⁴ There were some higher-molecular-weight polymers left after Soxlet purification, which were extracted out by chlorobenzene. Our result indicates that this method can synthesize graft polymers with a higher DP if there are no solubility issues. The average molecular weights of the two polymers were compared, and it showed a significant increase in $M_{\rm w}$ from 16.9 to 102 kg/mol. Further evidence from elemental analysis and NMR (Figure S7) confirmed that the components of the monomer 6 were indeed found in the polymer BP. Elemental analysis was in good agreement with the theoretical data: it was found that the N content of BP is 0.57% as it is supposed to be, while it is 0% for MM.

2.2. Optical Properties. The photophysical properties of the two polymers (MM and BP) were investigated using ultraviolet—visible (UV—vis) spectroscopy. The key physical properties are summarized in Table 2. Both of our polymers showed a very similar absorption spectrum from 300 to 500 nm in the visible region (Figure 2). This is very similar to that

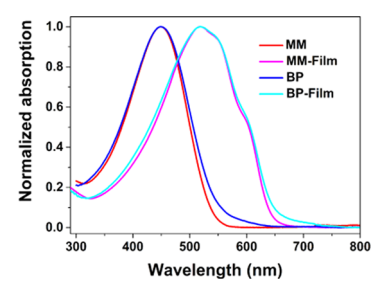


Figure 2. UV—vis absorption spectra of the copolymers in the film states.

of regioregular P3HT.¹⁶ The two polymers showed the same absorption maxima at 448 nm. Since the content of the backbone is relatively low compared to the P3HT side chains, backbone absorption might be overlapped with that of P3HT leading to almost identical spectra. Absorption maxima for thin films were shifted from 448 to 518 nm for both the polymers. The 70 nm red shift indicated a very strong aggregation in solid state, which is reasonable because the major component of the polymers is a regioregular¹⁷ P3HT chain.

2.3. Electrochemical Properties. Electrochemical spectra of the two polymers **MM** and **BP** were investigated by cyclic voltammetry (CV). The CV curves and their corresponding data (Figure 3 and Table 2) indicate that these polymers are

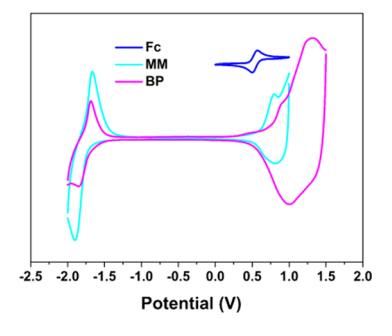


Figure 3. Cyclic voltammograms of polymers in $CH_3CN/0.1~M~Bu_4NPF_6$ at 50 mV/s.

electroactive. The redox potentials were first referenced to the ferrocene/ferrocenium redox couple (Fc/Fc $^+$), which is at 0.47 V vs a saturated calomel electrode (SCE). The redox potential of Fc/Fc $^+$ was then assumed to be at -4.8 eV relative to vacuum.

Table 2. Optical and Electrochemical Properties of the Two Copolymers

	solution $\lambda_{s,max}$ $(nm)^a$	film $\lambda_{f,max}$ (nm)	film λ_{edge} (nm)				
copolymers	Abs.	Abs.	Abs.	$E_{\rm g}^{\rm opt} \left({\rm eV}\right)^{b}$	HOMO (eV)	LUMO (eV)	$E_{\rm g}^{\rm \ ec}$ (eV)
MM	448	518	644	1.93	-4.95	-2.60	2.35
BP	448	518	649	1.91	-5.05	-2.66	2.39

[&]quot;Measured in a chloroform solution. "Band gap estimated from the optical absorption band edge of the films.

Then, the highest occupied molecular orbital (HOMO)/lowest unoccupied molecular orbital (LUMO) energy levels and electrochemical energy gaps ($E_{\rm g}^{\rm ec}$) of our copolymers were calculated as per the following equations

HOMO =
$$-(E_{ox} + 4.33)$$
 (eV)
LUMO = $-(E_{red} + 4.33)$ (eV)

$$E_{\rm g}^{\rm ec} = (E_{\rm ox} - E_{\rm red}) \, (\rm eV)$$

The onset oxidation potentials $(E_{\rm ox})$ were found to be 0.62 and 0.72 V for MM and BP, corresponding to the HOMO energy levels of -4.95 and -5.05 eV, respectively. The LUMO energy levels of MM and BP were calculated to be -2.60 and -2.66 eV, indicating a low band gap of 2.35 and 2.39 eV, respectively. The optical band gaps were calculated from their film absorption, and they were found to be 1.93 eV for MM and 1.91 eV for BP. It did not show large differences in electrochemical properties, which is reasonable because the P3HT side chains of the polymers contributed much more than the backbones. Therefore, the final properties were found to be the same as the properties of P3HT side chains.

2.4. Morphology Investigation. To investigate the morphology and packing of this graft polymer BP, grazing incidence wide-angle X-ray scattering two-dimensional (GI-WAXS-2D) was measured for the polymer films (Figure 4).

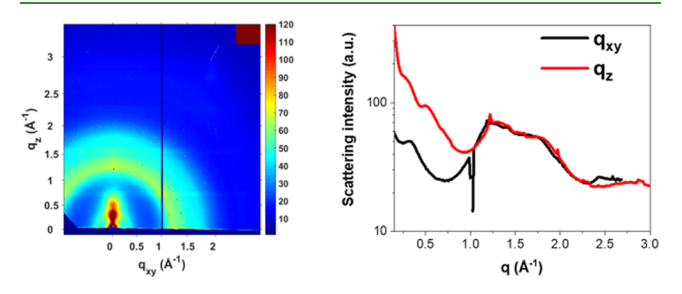


Figure 4. Two-dimensional GIWAXS scattering patterns of **BP** films (left) and one-dimensional (1D)-linecuts in out-of-plane (q_z) direction and in-plane (q_{sy}) direction (right).

The polymer films were coated onto the polished side of a silicon wafer. The polymer shows a broad arc scattering profile, corresponding to π – π stacking, which indicates the amorphous nature of the polymer. Unlike, P3HT, which has an edge-on orientation and exhibits sharp out-of-plane (100), (200), and (300) scattering peaks, this polymer exhibits no such peaks. In out-of-plane q_z direction, the polymer exhibits broad peaks at 0.3 and 0.5 Å⁻¹, corresponding to the distances 20.9 and 12.5 Å⁻¹, respectively./

2.5. Faraday Effect. To corroborate the results obtained from UV-visible spectroscopy and GIWAXS measurements, we employed magneto-optical polarimetry on these samples, as this technique is highly sensitive to morphology and stacking of P3HT materials. Magneto-optical activity was measured using a Faraday polarimeter under a low-frequency AC magnetic field through simultaneous balanced detection and homodyne detection (Figure S1). A full description of our instrument is found in the Supporting Information. Measurements were performed using a 532 nm coherent light source and measured in triplicate at five different field strengths across three separate thin-film samples of **BP**. High-quality thin films of **BP** (formed from spin coating; 81.8 ± 2.8 nm, measured by atomic force microscopy (AFM)) exhibited a Verdet constant

of 2.39 \pm 0.57 (10⁴) °/T·m (Table 3). Since these polymers contain P3HT brushes, it is appropriate to make similar

Table 3. Measured Verdet Constant and Faraday Rotation of BP and Related Materials

	verdet constant $(10^{4\circ}/\mathrm{T\cdot m})$	thickness (µm)	rotation at 148G (μ deg)
substrate	0.0292 ± 0.00025	1000 ± 3^a	841 ± 20
BP	2.4 ± 0.6	0.0818 ± 0.0028^{b}	32 ± 9
polystyrene	0.0167 ± 0.0010	10.0 ± 0.2^{c}	21 ± 3
RRP3HT	4.3 ± 1.5	0.108 ± 0.017^{c}	67 ± 23

^aMeasured by precision micron calipers. ^bDetermined by AFM. ^cDetermined by profilimeter.

measurements on RRP3HT for comparison and to reveal additional details on the morphology. Gangopadhyay and Persoons reported a Verdet Constant for RRP3HT of 6.25 ± 0.3 (10⁴) $^{\circ}$ /T·m, employing a similar instrumental method. $^{\overline{12}}$ In our laboratory, we obtained a Verdet Constant of 4.32 ± 1.5 (10⁴) °/T⋅m for RRP3HT in good agreement with this literature report. These data suggest that BP forms a structure similar to that of RRP3HT. Indeed, thermally annealed thin films of RRP3HT do not exhibit a Faraday effect or magnetooptical activity. The preservation of the magneto-optical effect in BP suggests that the RRP3HT side chains form extended, disordered domains, which is corroborated by the 2D GIWAXS measurements. Moreover, theory predicts that such domains should yield a Faraday response.²⁰ It is interesting to note that the inclusion of an acceptor moiety within the polymer backbone does not appear to yield a large perturbation on the magneto-optic activity of P3HT. Within the context of this sample, we thus infer that it is the RRP3HT brush units that are solely responsible for the rotation of planepolarized light in these studies. The precise origin of the Faraday effect in these materials is still an open question; however, since it is a diamagnetic material of low symmetry, the magneto-optic activity must arise through Faraday Bterms.²¹ This particular Faraday term quantifies optical activity attributed to a magnetic field-induced mixing of nondegenerate electronic states. This theoretical basis combined with the strong dependence on regioregularity and sample processing implicates the mixing of electronic states localized on closepacked RRP3HT chains.

3. CONCLUSIONS

In conclusion, we have demonstrated a finely designed grafting through approach for synthesizing fully conjugated graft polymers. A tin contained initiator was used for the synthesis of macromonomers (MM) by employing Kumada catalyst transfer polycondensation. The content of the trimethyltin functional group was precisely determined, which lead to good control of the 1:1 monomer ratio for the later copolymerization to obtain a graft polymer (BP). The structures of the newly developed polymers were characterized and analyzed, and experimental results were in good agreement with theoretical ones. The optical and electrochemical properties were studied, which were found to be the same as those of the P3HT side chains. The Faraday effect of BP was investigated, and it was found to be in accord with that exhibited by RRP3HT. Based on this result, we infer that the acceptor backbone permits the P3HT brush units to form a similar mesoscale structure to that displayed by RRP3HT. As more "graft-through" type polymers are produced through selective chemical functionalization, Faraday activity can serve as a reporter on the morphological characteristics of the RRP3HT side chains and their electronic coupling to the acceptor moieties in the polymer backbone. This work thus provides a simple and effective method for synthesizing fully conjugated graft polymers and to explore new properties and applications of these systems.

4. EXPERIMENTAL SECTION

¹H NMR and ¹³C NMR spectra were recorded on a Bruker DRX-500 spectrometer. Matrix-assisted laser desorption ionization time-of-flight (MALDI-TOF) mass spectra were recorded using a Bruker Ultraflextreme MALDI-TOF mass spectrometer with dithranol as the ionization matrix. Gas chromatography-mass spectra (GC-MS) were measured with Agilent SQ GC-MS (5977A single quad MS and 7890B GC). Ultraviolet-visible-near infrared (UV-vis-NIR) spectra of the polymers were measured on a SHIMADZU UV-3600 spectrometer. The elemental analyses of the polymers were performed on an Elementar Vario EL III element analyzer for C, H, Br, and S determination. Thermogravimetric analyses (TGA) were performed under nitrogen at a heating rate of 10 °C min⁻¹ using a SHIMADZU TGA-50 analyzer. The average molecular weight and polydispersity index (D) of the polymers were determined using Waters 1515 gel permeation chromatography (GPC) analysis with CHCl₃ as eluent and polystyrene as standard; there are two detectors for the instrument, refractive index detector and UV-vis detector; in this study, all of the molecular weights were collected from the traces with the UV-vis detector. Electrochemical redox potentials were obtained by cyclic voltammetry (CV) using a three-electrode configuration and an electrochemistry workstation (AUTOLAB PGSTAT12). CV was conducted on an electrochemistry workstation with the polymer thin film on a Pt working electrode, Pt as the counter electrode as well, and Ag/AgCl as a reference electrode in a 0.1 M tetra-n-butylammonium hexafluorophosphate acetonitrile solution at a scan rate of 50 mV s⁻¹. ICP-MS data was obtained with an Agilent 7700x ICP-MS and analyzed using ICP-MS MassHunter version B01.03. A commercially available standard E2-TB01060 from the company Inorganic Ventures was used. Ten milligrams of vacuum-dried sample was weighed in a glass vial. One milliliter of metal-free 70% nitric acid was added to each vial and then incubated on 80 °C water bath for 3 h until all solid samples dissolved. The digested sample in 70% nitric acid was diluted 35 times by DI water to prepare a 2% nitric acid solution; then, further diluted by 2% nitric acid until the ICP-MS read out below 500 ppb. Faraday rotation was detected using a homodyne detection scheme. A 532 nm diode laser was initially polarized at 45°. This light was directed through a thin-film sample mounted in the center of a solenoid. The reference frequency generated by a Stanford research instruments SR830 lock-in amplifier was further amplified and used to generate a low-frequency magnetic field. The polarizing beam splitter positioned after the sample converts changes in polarization into intensity changes in two beams, which are then detected by a Newport nirvana 2007 balanced detection system (Figure S1). Multiple measurements are made while incrementally increasing the magnetic field generated by the solenoid, and a Verdet constant is extracted by fitting polarization measurements against magnetic field measurements using a least-squares linear regression.

ASSOCIATED CONTENT

Supporting Information

The Supporting Information is available free of charge at https://pubs.acs.org/doi/10.1021/acsami.0c08170.

It includes a detailed synthesis of the monomers and polymers; characterization methods (PDF)

AUTHOR INFORMATION

Corresponding Authors

Jeffrey J. Rack — Department of Chemistry and Chemical Biology, Laboratory for Magneto-Optic Spectroscopy, University of New Mexico, Albuquerque, New Mexico 87131, United States; orcid.org/0000-0001-6121-879X; Email: jrack@unm.edu

Luping Yu — Department of Chemistry and The James Franck Institute, The University of Chicago, Chicago, Illinois 60637, United States; Email: lupingyu@uchicago.edu

Authors

Xunshan Liu − Department of Chemistry and The James Franck Institute, The University of Chicago, Chicago, Illinois 60637, United States; oorcid.org/0000-0003-1537-258X

Emigdio E. Turner — Department of Chemistry and Chemical Biology, Laboratory for Magneto-Optic Spectroscopy, University of New Mexico, Albuquerque, New Mexico 87131, United States

Valerii Sharapov — Department of Chemistry and The James Franck Institute, The University of Chicago, Chicago, Illinois 60637, United States; o orcid.org/0000-0002-2828-0468

Dafei Yuan — Department of Chemistry and The James Franck Institute, The University of Chicago, Chicago, Illinois 60637, United States; orcid.org/0000-0001-5914-2060

Mohammad A. Awais – Department of Chemistry and The James Franck Institute, The University of Chicago, Chicago, Illinois 60637, United States

Complete contact information is available at: https://pubs.acs.org/10.1021/acsami.0c08170

Notes

The authors declare no competing financial interest.

ACKNOWLEDGMENTS

This work was supported by NSF (Chem-1802274), partially supported by the University of Chicago Materials Research Science and Engineering Center, which is funded by the National Science Foundation under award number DMR-1420709. This research used resources of the Advanced Photon Source, a U.S. Department of Energy (DOE) Office of Science User Facility operated for the DOE Office of Science by Argonne National Laboratory under Contract No. DE-AC02-06CH11357. We thank Wenbo Han for the ICP-MS measurements. J.J.R. acknowledges NSF (CHE-1856492) for support of this work. E.E.T. acknowledges the NSF for a Graduate Research Fellowship Program for support (DGE-1418062).

REFERENCES

- (1) Wu, W.; Liu, Y.; Zhu, D. π -Conjugated Molecules with Fused Rings for Organic Field-effect Transistors: Design, Synthesis and Applications. *Chem. Soc. Rev.* **2010**, *39*, 1489–1502.
- (2) Wang, C.; Dong, H.; Jiang, L.; Hu, W. Organic Semiconductor Crystals. Chem. Soc. Rev. 2018, 47, 422–500.
- (3) Lu, L.; Zheng, T.; Wu, Q.; Schneider, A. M.; Zhao, D.; Yu, L. Recent Advances in Bulk Heterojunction Polymer Solar Cells. *Chem. Rev.* **2015**, *115*, 12666–12731.
- (4) Zeigler, D. F.; Mazzio, K. A.; Luscombe, C. K. Fully Conjugated Graft Copolymers Comprising a P-Type Donor—Acceptor Backbone and Poly(3-hexylthiophene) Side Chains Synthesized Via a "Graft Through" Approach. *Macromolecules* **2014**, *47*, 5019–5028.
- (5) Wang, J.; Lu, C.; Mizobe, T.; Ueda, M.; Chen, W.-C.; Higashihara, T. Synthesis and Characterization of All-Conjugated

- Graft Copolymers Comprised of n-Type or p-Type Backbones and Poly(3-hexylthiophene) Side Chains. *Macromolecules* **2013**, *46*, 1783–1793.
- (6) Riera-Galindo, S.; Leonardi, F.; Pfattner, R.; Mas-Torrent, M. Organic Semiconductor/Polymer Blend Films for Organic Field-Effect Transistors. *Adv. Mater. Technol.* **2019**, *4*, No. 1900104.
- (7) Wang, G.; Swick, S. M.; Matta, M.; Mukherjee, S.; Strzalka, J. W.; Logsdon, J. L.; Fabiano, S.; Huang, W.; Aldrich, T. J.; Yang, T.; Timalsina, A.; Powers-Riggs, N.; Alzola, J. M.; Young, R. M.; DeLongchamp, D. M.; Wasielewski, M. R.; Kohlstedt, K. L.; Schatz, G. C.; Melkonyan, F. S.; Facchetti, A.; Marks, T. J. Photovoltaic Blend Microstructure for High Efficiency Post-Fullerene Solar Cells. To Tilt or Not To Tilt? J. Am. Chem. Soc. 2019, 141, 13410–13420.
- (8) Hwang, Y.-J.; Earmme, T.; Courtright, B. A. E.; Eberle, F. N.; Jenekhe, S. A. n-Type Semiconducting Naphthalene Diimide-Perylene Diimide Copolymers: Controlling Crystallinity, Blend Morphology, and Compatibility toward High-performance All-Polymer Solar Cells. *J. Am. Chem. Soc.* **2015**, *137*, 4424–4434.
- (9) Chatterjee, S.; Karam, T. E.; Rosu, C.; Wang, C.-H.; Youm, S. G.; Li, X.; Do, C.; Losovyj, Y.; Russo, P. S.; Haber, L. H.; Nesterov, E. E. Silica—Conjugated Polymer Hybrid Fluorescent Nanoparticles: Preparation by Surface-Initiated Polymerization and Spectroscopic Studies. *J. Phys. Chem. C* **2018**, *122*, 6963—6975.
- (10) Khanduyeva, N.; Senkovskyy, V.; Beryozkina, T.; Bocharova, V.; Simon, F.; Nitschke, M.; Stamm, M.; Grötzschel, R.; Kiriy, A. Grafting of Poly(3-hexylthiophene) from Poly(4-bromostyrene) Films by Kumada Catalyst-Transfer Polycondensation: Revealing of the Composite Films Structure. *Macromolecules* **2008**, *41*, 7383–7389.
- (11) Lutz, J. P.; Hannigan, M. D.; McNeil, A. J. Polymers Synthesized via Catalyst-transfer Polymerization and Their Applications. *Coord. Chem. Rev.* **2018**, *376*, 225–247.
- (12) Gangopadhyay, P.; Voorakaranam, R.; Lopez-Santiago, A.; Foerier, S.; Thomas, J.; Norwood, R. A.; Persoons, A.; Peyghambarian, N. Faraday Rotation Measurements on Thin Films of Regioregular Alkyl-Substituted Polythiophene Derivatives. *J Phys. Chem. C* 2008, *112*, 8032–8037.
- (13) Araoka, F.; Abe, M.; Yamamoto, T.; Takezoe, H. Large Faraday Rotation in a π -Conjugated Poly(arylene ethynylene) Thin Film. *Appl. Phys. Express* **2009**, *2*, No. 011501.
- (14) Koeckelberghs, G.; Vangheluwe, M.; Doorsselaere, K. V.; Robijns, E.; Persoons, A.; Verbiest, T. Regioregularity in Poly(3-alkoxythiophene)s: Effects on the Faraday Rotation and Polymerization Mechanism. *Macromol. Rapid Commun.* **2006**, *27*, 1920–1925.
- (15) Gangopadhyay, P.; Koeckelberghs, G.; Persoons, A. Magneto-optic Properties of Regioregular Polyalkylthiophenes. *Chem. Mater.* **2011**, 23, 516–521.
- (16) Fei, Z.; Boufflet, P.; Wood, S.; Wade, J.; Moriarty, J.; Gann, E.; Ratcliff, E. L.; McNeill, C. R.; Sirringhaus, H.; Kim, J.-S.; Heeney, M. Influence of Backbone Fluorination in Regioregular Poly(3-alkyl-4-fluoro)thiophenes. *J. Am. Chem. Soc.* **2015**, *137*, 6866–6879.
- (17) Yuan, M.; Okamoto, K.; Bronstein, H. A.; Luscombe, C. K. Constructing Regioregular Star Poly(3-hexylthiophene) via Externally Initiated Kumada Catalyst-Transfer Polycondensation. *ACS Macro Lett.* **2012**, *1*, 392–395.
- (18) Wang, M.; Hu, X.; Liu, P.; Li, W.; Gong, X.; Huang, F.; Cao, Y. Donor-acceptor Conjugated Polymer Based on Naphtho[1,2-c:5,6-c]bis[1,2,5]thiadiazole for High-performance Polymer Solar cells. J. Am. Chem. Soc. 2011, 133, 9638–9641.
- (19) Chang, C.-Y.; Wang, L.; Shy, J.-T.; Lin, C.-E.; Chou, C. Sensitive Faraday Rotation Measurement with Auto-balanced Photo-detection. *Rev. Sci. Instrum.* **2011**, 82, No. 063112.
- (20) Louant, O.; Liégeois, V.; Verbiest, T.; Persoons, A.; Champagne, B. Faraday Effect in Stacks of Aromatic Molecules. *J. Phys. Chem. C* **2017**, *121*, 15348–15352.
- (21) Barron, L. D. Molecular Light Scattering and Optical Activity, 2nd ed.; Cambridge University Press: Cambridge, 2004.